

Relative production rates of ${}^6\text{He}$, ${}^9\text{Be}$, ${}^{12}\text{C}$ in astrophysical environments

R. de Diego and E. Garrido

Instituto de Estructura de la Materia, CSIC, Serrano 123, E-28006 Madrid, Spain

D.V. Fedorov and A.S. Jensen

Department of Physics and Astronomy, Aarhus University, DK-8000 Aarhus C, Denmark

(Dated: July 23, 2018)

We assume an environment of neutrons and α -particles of given density and temperature where nuclear syntheses into ${}^6\text{He}$, ${}^9\text{Be}$ and ${}^{12}\text{C}$ are possible. We investigate the resulting relative abundance as a function of density and temperature. When the relative abundance of α -particles Y_α is between 0.2 and 0.9, or larger than 0.9, the largest production is ${}^9\text{Be}$ or ${}^{12}\text{C}$, respectively. When $Y_\alpha < 0.2$ ${}^6\text{He}$ is mostly frequently produced for temperatures above about 2 GK whereas the ${}^9\text{Be}$ production dominates at smaller temperatures.

PACS numbers: 25.10.+s, 25.40.Lw, 26.30.Hj

Introduction. Formation of heavy elements must overcome the problem that all nuclear isotopes with mass numbers 5 and 8 are unstable [1]. As a consequence, once the hydrogen fuel in a star is exhausted, the production of energy by formation of ${}^4\text{He}$ stops and the temperature drops. The subsequent gravitational collapse increases the temperature, and the red giant phase, where helium is now the source of energy, begins. Due to the lack of neutrons in the core of the helium burning red giants, the $A=5$ and $A=8$ instability gaps have to be bridged by the triple-alpha reaction $\alpha + \alpha + \alpha \rightarrow {}^{12}\text{C} + \gamma$, which is the most relevant one in stars at the helium burning stage.

Nevertheless, at conditions of high alpha and neutron densities, the reactions $\alpha + n + n \rightarrow {}^6\text{He} + \gamma$ and $\alpha + \alpha + n \rightarrow {}^9\text{Be} + \gamma$ are also possible, and they will play a role in bridging the $A = 5, 8$ gaps. As described in [1–3], such a scenario can appear at the early Big Bang stages or in the nucleosynthesis related to the type II supernova shock front. In both cases, temperatures are estimated to be of about 7 to 10 GK (1 GK=10⁹ K).

The dominating process is in any case the electromagnetic radiative recombination of the three particles from continuum to bound state, except at very high densities where four-body recombination can compete favorably [4]. However, the three-body processes producing these nuclei differ from each other. In particular, the production of ${}^6\text{He}$ and ${}^9\text{Be}$ is dominated by dipole transitions, while the production of ${}^{12}\text{C}$ is of quadrupole character.

The three-body processes described above are usually treated as two-step processes where the unstable isotopes ${}^5\text{He}$ and ${}^8\text{Be}$ first are created and second, before decaying, react with another neutron or α -particle [5–7]. This approximation of two independent sequential processes does not provide an accurate description since the lifetimes of the intermediate configurations are comparable to, or shorter than, the reaction time of the last step of the process [8]. This implies that the processes proceed through genuine three-body reactions.

The approximations employed to overcome this difficulty are, almost always, extensions of the bare two-step model where the finite lifetime, or width, of the reso-

nances is incorporated into the description [9]. The fact that this can be tremendously wrong was discussed recently in a full three-body calculation of the triple α -process at very low energies. In [10] an increase in the triple alpha reaction rate by about 20 orders of magnitude around 10⁷ K compared with the rate in [11] was found. In [12] it is shown that such an increase is incompatible with observations of extended red giant branches and He burning stars in old stellar systems. The three-body character is in general crucial for resonance structure calculations [13, 14] and the related dynamic evolution describing the decay mechanism [14–16].

The correct three-body calculations are technically difficult because they involve the continuum dynamics of three particles interacting via a mixture of short and long-range forces. Only recently it has become feasible to perform general three-body computations with the correct boundary conditions at both small and large distances, and where no assumption is made about the capture mechanism (sequential or direct).

The purpose of the present letter is to investigate the only possible three-particle reactions at conditions of high alpha and neutron density. The novelty of this work is that we are doing it using a three-body method that is not making any assumption about the reaction mechanism. In this way, we shall investigate the relative abundances of the three nuclei, ${}^6\text{He}$, ${}^9\text{Be}$ and ${}^{12}\text{C}$, created from neutrons and α -particles at given densities and temperatures. The conditions under which the production of each nucleus is the dominant process will be established.

Formulation. We consider radiative capture of three particles, (abc) , into a bound nucleus A of binding energy B_A , i.e. $a + b + c \rightarrow A + \gamma$. The particles are α -particles and neutrons in various combinations. The corresponding reaction rate $R_{abc}(E)$ can be related to the inverse process of photodissociation. Eq.(20) in [17] gives the ratio between the “energy averaged” reaction rates for the processes $a + b + c \leftrightarrow A + d$. Making use of (32) in [17] and specializing to the case in which d is a photon, one

can identify the relation:

$$R_{abc}(E) = \frac{\hbar^3}{c^2} \frac{8\pi}{(\mu_x \mu_y)^{3/2}} \left(\frac{E_\gamma}{E} \right)^2 \frac{2g_A}{g_a g_b g_c} \sigma_\gamma(E_\gamma) \quad (1)$$

where $E = E_\gamma + B_A$ is the initial three-body kinetic energy, E_γ is the photon energy, $\sigma_\gamma(E_\gamma)$ is the photo dissociation cross section of the A nucleus, c is the velocity of light, g_i is the degeneracy of particle $i = a, b, c, A$, and μ_x and μ_y are the reduced masses of the systems related to the Jacobi coordinates, (\mathbf{x}, \mathbf{y}) , for the three-body system [18].

The production rate P for the capture reaction is obtained after averaging $R_{abc}(E)$ using the Maxwell-Boltzmann distribution as weighting function, and multiplying by the density n_i of particles a, b , and c . This density is usually written as $n_i = \rho N_A X_i / A_i$, where ρ is the density of the environment, N_A is the Avogadro number, A_i is the mass number of particle i , and $X_i = N_i M_i / (N_a M_a + N_b M_b + N_c M_c)$ is the mass abundance of nucleus i expressed by the number of particles N_i and their masses M_i (see Eqs.(1) and (3) in ([17])). It is also possible to use the relative abundance defined by $Y_i = N_i / (N_a + N_b + N_c)$.

In this way the final expression for the production rate P depends then on both, temperature (T) and mass density (ρ) of the environment, which can vary substantially in different scenarios, and it takes the form [17]:

$$P_{abc}(\rho, T) = n_a n_b n_c \frac{\hbar^3}{c^2} \frac{8\pi}{(\mu_x \mu_y)^{3/2}} \frac{g_A}{g_a g_b g_c} e^{-\frac{B}{k_B T}} \times \frac{1}{(k_B T)^3} \int_{|B|}^{\infty} E_\gamma^2 \sigma_\gamma(E_\gamma) e^{-\frac{E_\gamma}{k_B T}} dE_\gamma. \quad (2)$$

The photodissociation cross section for the inverse process $A + \gamma \rightarrow a + b + c$ can be expanded into electric and magnetic multipoles. In particular, the electric multipole contribution of order λ has the form [19]:

$$\sigma_\gamma^{(\lambda)}(E_\gamma) = \frac{(2\pi)^3 (\lambda + 1)}{\lambda [(2\lambda + 1)!!]^2} \left(\frac{E_\gamma}{\hbar c} \right)^{2\lambda - 1} \frac{d\mathcal{B}}{dE}, \quad (3)$$

where the strength function \mathcal{B} is

$$\mathcal{B}(E\lambda, n_0 J_0 \rightarrow n J) = \sum_{\mu M} |\langle n J M | O_\mu^\lambda | n_0 J_0 M_0 \rangle|^2, \quad (4)$$

where J_0, J and M_0, M are the total angular momenta and their projections of the initial and final states, and all the other needed quantum numbers are collected into n_0 and n . The electric multipole operator is given by:

$$O_\mu^\lambda = \sum_{i=1}^3 z_i |\mathbf{r}_i - \mathbf{R}|^\lambda Y_{\lambda, \mu}(\Omega_{y_i}), \quad (5)$$

where i runs over the three particles, and where we neglect contributions from intrinsic transitions within each of the three constituents [20].

Test of the method. The crucial strength function, \mathcal{B} , is computed by genuine three-body calculations of both the bound final state and the continuum initial states. We have used the hyperspherical adiabatic expansion method described in [18]. The n - n , α - n , and α - α interactions are the ones given in [14, 21]. The basic procedure is computation of three-body states of given angular momentum and parity confined by box boundary conditions [22]. In this way the continuum spectrum is discretized. The strength functions are then obtained for each discrete continuum state according to Eq.(4). The distribution $d\mathcal{B}/dE$ is built by use of the finite energy interval approximation, where the energy range is divided into bins, and all the discrete values of \mathcal{B} falling into a given bin are added. Afterwards the points are connected by spline operations and the expressions (3) and (2) are computed.

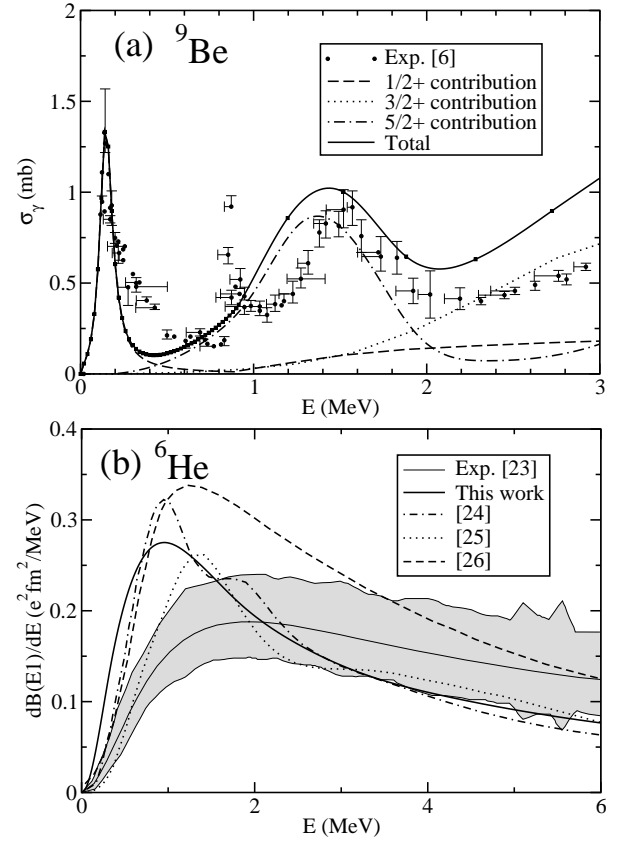


FIG. 1: (a) Photodissociation cross section for ${}^9\text{Be}$. The total computed cross section is given by the solid line. The contributions from transitions to the $1/2^+$, $3/2^+$, and $5/2^+$ continuum three-body states are given by the dashed, dotted, and dot-dashed curves, respectively. The experimental data are from [6]. (b) Comparison between different computed dipole strength functions for ${}^6\text{He}$ and the experimental data (shaded area) from [23].

In the upper part of Fig.1 we show the computed photodissociation cross section of ${}^9\text{Be}$. The experimental data in the figure are from [6]. The dashed, dotted, and dot-dashed curves give the contribution to the transition

strength in Eq.(4), and therefore to the total cross section (solid line), from the $\alpha + \alpha + n$ continuum states with total spin and parity $1/2^+$, $3/2^+$, and $5/2^+$, respectively (the ground state in ${}^9\text{Be}$ has spin and parity $3/2^-$). As seen in the figure, the agreement with the experiment is reasonably good, except for energies above 2 MeV, where the computed cross section clearly overestimates the experimental data. This is because the interaction used in the three-body calculation provides a $3/2^+$ resonance twice wider than the experimental one. The narrow peak at 0.9 MeV is a known $5/2^-$ resonance which can only be populated through the M1 transition which is neglected in this calculation.

For ${}^6\text{He}$, our computed dB/dE (thick solid line in the figure) agrees reasonably well with the previous calculations in [24, 25]. The one in [26] gives clearly larger values, mainly for energies beyond 1 MeV. In any case, none of the calculations fits well the experimental data (thin solid line) for all the energies despite the large experimental error bars. All the calculations show a sharp enhancement in the low energy region which is not seen in the experiment. Further experimental data would help to clarify this issue. In similar measurements with ${}^{11}\text{Li}$, the peak in the experimental strength function moved to lower energies [27, 28], and thus closer to our theoretical predictions [29], after improvements in the detection of the low energy neutrons.

Density dependence. The density dependence of the production rates in Eq.(2) is very simple for a given temperature. The basic reaction rate for only three particles has to be multiplied by the number of each species of particles. For a given total density ρ found by adding neutron and α -particle densities we can express the density dependence as $\rho^3 X_\alpha^n X_n^{3-n}$, where $X_n = 1 - X_\alpha$ and X_α are the mass fraction of neutrons and α -particles. Then $n = 1, 2, 3$ correspond to production of ${}^6\text{He}$, ${}^9\text{Be}$ and ${}^{12}\text{C}$, respectively.

When no α -particles are present, $X_\alpha = Y_\alpha = 0$, the production rates are all zero. When only α -particles are present, $X_\alpha = Y_\alpha = 1$, only ${}^{12}\text{C}$ can be produced. The density dependence for production of ${}^6\text{He}$ and ${}^9\text{Be}$ are each others reflection in $X_\alpha = 1/2$ but pushed towards smaller values as function of Y_α . The production of ${}^{12}\text{C}$ increases monotonically as function of X_α and Y_α .

Temperature dependence. The temperature dependence is obtained by folding the calculated energy dependence with the Boltzmann distribution as seen formally in Eq.(2) and shown numerically in Fig.2. We show results from about 0.1 GK to 10 GK. The lower limit is where we run out of accuracy due to the present discretization method, and the upper limit allows inclusion of the relevant processes. For completeness we discuss the behavior in the full interval. The three-body processes producing the three nuclei, ${}^6\text{He}$, ${}^9\text{Be}$, ${}^{12}\text{C}$, differ from each other. Two neutrons and one α -particle produce the 0^+ ground state of ${}^6\text{He}$ by electromagnetic recombination where one photon emerges with total angular momentum and parity $J^\pi = 1^-, 2^+$. The dipole

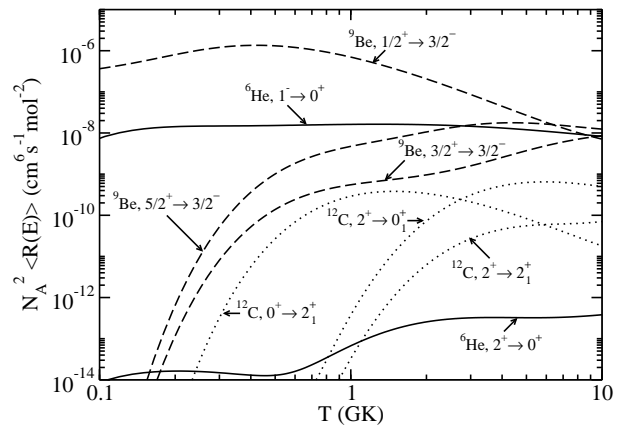


FIG. 2: The rates as functions of temperature for producing ${}^6\text{He}$, ${}^9\text{Be}$ and ${}^{12}\text{C}$ in their respective ground states from various continuum states. From 1^- and 2^+ to 0^+ for ${}^6\text{He}$ (solid curves), from $1/2^+$, $3/2^+$, and $5/2^+$ to $3/2^-$ for ${}^9\text{Be}$ (dashed curves), from 2^+ to the 0^+ ground state and from both 0^+ and 2^+ to 2^+ excited bound state for ${}^{12}\text{C}$ (dotted curves).

transition is strongly preferred in spite of the low-lying 2^+ three-body resonance in ${}^6\text{He}$ [4, 22].

One neutron and two α -particles in continuum states of $J^\pi = 1/2^+, 3/2^+, 5/2^+$ combine directly by dipole transitions into the $3/2^-$ ground state of ${}^9\text{Be}$. Resonances enhance the transitions in various energy ranges. At low temperature transitions from the $1/2^+$ state dominate by several orders of magnitude but at $T \approx 5$ GK the $5/2^+$ transition has almost reached the same value, see Fig.2. This behavior is related to the corresponding resonances at excitation energies of 1.68 MeV and 3.05 MeV, respectively. The $3/2^+$ resonance is located at a much higher energy and the corresponding transition always remains smaller. Furthermore, higher multipoles give insignificant contributions at these temperatures [4].

Three α -particles can combine into the ground state of ${}^{12}\text{C}$ through several paths. At low temperature the quadrupole transitions from 0^+ dominates due to the Hoyle resonance, but the quadrupole transition from the 2^+ continuum to the ground state increases and begin to dominate at $T \approx 2.5$ GK, see Fig.2. The precise value depends on the energy of the lowest 2^+ resonance which here was assumed to be 1.38 MeV above the three-body threshold [14]. The remaining quadrupole transition from 2^+ to 2^+ is smaller for all temperatures.

All these transitions are compared in Fig.2. The production rate for ${}^9\text{Be}$ is by far the largest at low temperatures but matched for ${}^6\text{He}$ above temperatures of $T \approx 8$ GK. The rate for production ${}^{12}\text{C}$ is much smaller in this temperature range.

In Fig.3 the total reaction rates in Fig.2 are compared with previous calculations. The computed rates for ${}^6\text{He}$, ${}^9\text{Be}$, and ${}^{12}\text{C}$ are given by the dashed, solid, and dotted curves, respectively. In [3] the reaction rate for production of ${}^6\text{He}$ is given by assuming a sequential capture process through the $3/2^-$ resonance in ${}^5\text{He}$. This reac-

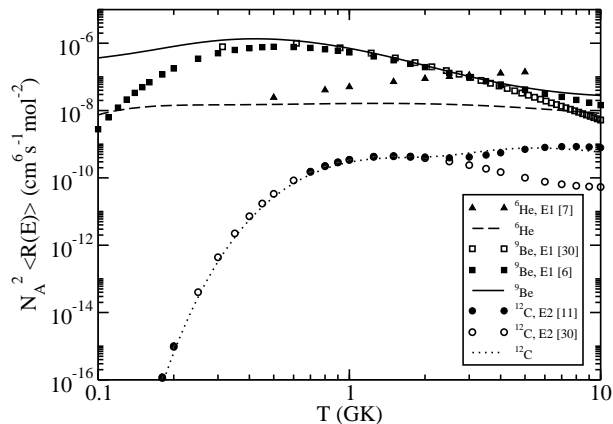


FIG. 3: Comparison between the total computed rates for production of ${}^6\text{He}$ (dashed line), ${}^9\text{Be}$, (solid line), and ${}^{12}\text{C}$ (dotted line) and the ones calculated in [7] for ${}^6\text{He}$, in [6, 30] for ${}^9\text{Be}$, and in [11, 30] for ${}^{12}\text{C}$.

tion rate is about three orders of magnitude smaller than our calculation, where the sequential capture assumption has not been made. In [7] they give the same reaction rate but adding the contribution of a dineutron capture. This is shown by the closed triangles in the figure, which now an order of magnitude *above* our calculation.

For production of ${}^9\text{Be}$, our reaction rate agrees well with the ones in Refs.[30] (open squares) and [6] (closed squares) for temperatures above 1 GK. Below this temperature our reaction rate is clearly bigger. For ${}^{12}\text{C}$ our computed rate agrees very well with the results given in [11, 30], where a sequential capture through the narrow 0^+ resonance in ${}^8\text{Be}$ is assumed. The agreement with [11] (closed circles) is particularly good. The deviations from [30] (open circles) arise because we include the contribution from the $2^+ \rightarrow 0^+$ transitions which is responsible for the enhancement of the tail for temperatures above 3 GK (see the dotted curves in Fig.2). The good agreement with [11] does not imply that we disagree with the spectacular results in [10] where huge enhancements of the reaction rates are reported for energies around 0.01 GK. We only discuss temperatures down to 0.1 GK where the present method is applicable. However, we see no indication of such rate increase at very low temperature.

Density-temperature dependence. The complicated temperature dependence in Fig.2 can now be combined with the simple density dependence, $n_a n_b n_c$, in Eq.(2). After adding up the different contributions for each of the three nuclei we find the creation probabilities as functions of temperature for three different relative fractions of the three nuclei. Creation of ${}^{12}\text{C}$ only becomes competitive for any temperature when Y_α is close to unity, i.e. when essentially only α -particles are present.

The slightly increasing ${}^6\text{He}$ curves cross the slightly decreasing ${}^9\text{Be}$ curves while the ${}^{12}\text{C}$ curves stay below for all temperatures below 10 GK. Thus unless the relative α -neutron abundance is extreme we get dominance of ${}^9\text{Be}$ at small temperature and dominance of ${}^6\text{He}$ at large tem-

perature. However, now it is important precisely which number of neutrons and α -particles are available for the recombination process. When $Y_\alpha = 0.1$ the dominance changes from ${}^9\text{Be}$ to ${}^6\text{He}$ at $T \approx 2.5$ GK. For Y_α values larger than 0.3 ${}^9\text{Be}$ dominates for all temperatures.

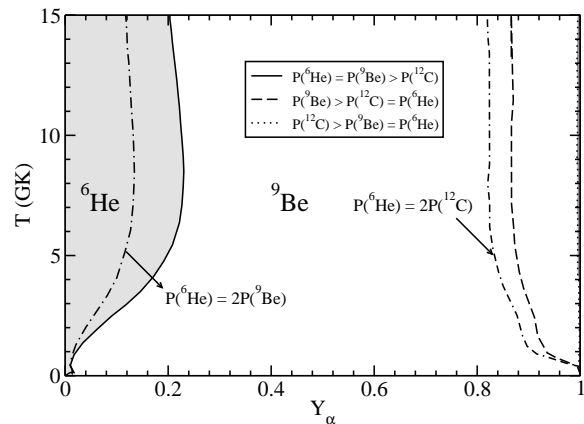


FIG. 4: The phase diagram for producing ${}^6\text{He}$, ${}^9\text{Be}$ and ${}^{12}\text{C}$ in the Y_α -temperature parameter space. The curves correspond to a constant ratio of production rates of two nuclei.

Relative production. The complete picture of the density-temperature dependence of the three-body reaction rates for creating the three nuclei is shown in Fig.4. All these nuclei can be destroyed in the same environment but we consider here only the individual three-body reactions creating them. Transfer reactions from ${}^6\text{He}$ and ${}^9\text{Be}$ using the same basic ingredients of neutrons and alphas can also produce ${}^9\text{Be}$ and ${}^{12}\text{C}$. However, we leave these four-body processes for future work, they are beyond the scope of the present investigation. For Y_α less than about 0.1 and temperatures above $T \approx 1-4$ GK the nucleus ${}^6\text{He}$ is produced more than twice as often as ${}^9\text{Be}$. As Y_α increases the relative ${}^9\text{Be}$ production increases and becomes dominant for all temperatures when Y_α exceeds 0.2.

By further increase of Y_α the relative creation rate of ${}^{12}\text{C}$ increases. At $Y_\alpha \approx 0.82$ the ${}^9\text{Be}$ production is still dominating when ${}^{12}\text{C}$ is created with half the rate of ${}^6\text{He}$. At $Y_\alpha \approx 0.86$ the production rates for ${}^{12}\text{C}$ and ${}^6\text{He}$ are equal, but the production of ${}^9\text{Be}$ still dominates. Only when Y_α is larger than about 0.99, where very few neutrons are present, the production rate of ${}^{12}\text{C}$ exceeds the other rates. These relative rates are very crudely independent of temperature except for very low Y_α values. Except for the small Y_α results, similar overall conclusions were obtained in previous investigations [3, 5, 31].

Summary and conclusions. We have compared calculated results of production rates of three-cluster nuclei, ${}^6\text{He}$, ${}^9\text{Be}$, ${}^{12}\text{C}$, consisting of neutrons and α -particles. The density and temperature dependence are investigated in a three-body model where the necessary continuum structures are treated by discretization in a large box. The two-body interactions are realistic and reproducing low-energy scattering properties. The position of

the lowest 2^+ resonance in ^{12}C is not precisely known but the results are rather insensitive to this energy. In general the results are very robust against variations within realistic limits of the interactions.

The ^{12}C production only dominates when the number of α -particles is 100 times larger than the number of neutrons. At lower relative α -particle density the ^9Be production is most frequent until ^6He begins to dominate when the number of α -particles is about 1/4 of the number of neutrons. An exception is low α -particle density and temperatures below about 2 GK where the ^9Be rate is largest. Thus the actual temperature is important when only relatively few α -particles are present.

The full implications of the present results require detailed numerical investigations of the sequences of processes leading to formation of heavier nuclei. The initial conditions in these related chains of reactions should be our relative production rates. Whether the outcome is consistent with observations of nuclear abundances remains to be seen.

Acknowledgments. This work was partly supported by funds provided by DGI of MEC (Spain) under contract No. FIS2008-01301. One of us (R.D.) acknowledges support by a Ph.D. I3P grant from CSIC and the European Social Fund.

-
- [1] A. Aprahamian, K. Langanke, M. Wiescher, Prog. Part. Nucl. Phys. 54, 535 (2005).
- [2] B.S. Meyer G.J. Mathews, W.M. Howard, S.E. Woosley, and R.D. Hoffman, Astrophys. J. 399, 656 (1992).
- [3] J. Görres, H. Herndl, I.J. Thompson, M. Wiescher, Phys. Rev. C 52, 2231 (1995).
- [4] R. de Diego, E. Garrido, D.V. Fedorov and A.S. Jensen, To be submitted for publication.
- [5] V.D. Efros, W. Balogh, H. Herndl, R. Hofinger, and H. Oberhummer, Z. Phys. A 355, 101 (1996).
- [6] K. Sumiyoshi, H. Utsunomiya, S. Goko, and T. Kajino, Nucl. Phys. A 709, 467 (2002).
- [7] A. Bartlett, J. Görres, G.J. Mathews, K. Otsuki, M. Wiescher, D. Frekers, A. Mengoni, and J. Tostevin, Phys. Rev. C 74, 015802 (2006).
- [8] H.O.U. Fynbo, R. Álvarez-Rodríguez, A.S. Jensen, O.S. Kirsebom, D.V. Fedorov, E. Garrido, Phys. Rev. C 79, 054009 (2009).
- [9] D. Baye and P. Descouvemont, Nucl. Phys. A 407, 77 (1983).
- [10] K. Ogata, M. Kan, M. Kamimura, Prog. Theor. Phys. 122, 1055 (2009).
- [11] C. Angulo et al., Nucl. Phys. A 656, 3 (1999).
- [12] A. Dotter and B. Paxton, Astron. Astrophys. 507, 1617 (2009).
- [13] D. V. Fedorov and A. S. Jensen, Phys. Lett. B 389, 631 (1996).
- [14] R. Alvarez-Rodriguez, E. Garrido, A.S. Jensen, D.V. Fedorov, and H.O.U. Fynbo, Eur.Phys.J. A 31, 303 (2007).
- [15] E. Garrido, D.V. Fedorov, A.S. Jensen, Phys.Lett. B 684, 132 (2010).
- [16] R. Álvarez-Rodríguez, A.S. Jensen, E. Garrido, D.V. Fedorov, H.O.U. Fynbo, Phys.Rev. C 77, 064305 (2008).
- [17] W. A. Fowler, G. R. Caughlan, and B. A. Zimmerman, Annu. Rev. Astron. Astrophys. 5, 525 (1967).
- [18] E. Nielsen, D.V. Fedorov, A.S. Jensen, and E. Garrido, Phys. Rep. 347, 373 (2001).
- [19] C. Forseén, N.B. Shul'gina, M.V. Zhukov, Phys. Rev. C 67, 045801 (2003).
- [20] C. Romero-Redondo, E. Garrido, D.V. Fedorov, and A.S. Jensen, Phys. Rev. C 77, 054313 (2008).
- [21] E. Garrido, D.V. Fedorov, A.S. Jensen, Nucl. Phys. A 700, 117 (2002).
- [22] R. de Diego, E. Garrido, D.V. Fedorov, A.S. Jensen, Phys. Rev. C 77, 024001 (2008).
- [23] T. Aumann et. al., Phys. Rev. C 59, 1252 (1999).
- [24] A. Cobis, D.V. Fedorov, A.S. Jensen, Phys. Rev. Lett. 79, 2411 (1997).
- [25] B.V. Danilin, I.J. Thompson, J.S. Vaagen, M.V. Zhukov, Nucl. Phys. A 632, 383 (1998).
- [26] T. Myo, K. Kato, S. Aoyama, and K. Ikeda, Phys.Rev. C 63, 054313 (2001).
- [27] S. Shimoura, T. Nakamura, M. Ishihara, N. Inabe, T. Kobayashi, T. Kubo, R.H. Siemssen, I. Tanihata, and Y. Watanabe, Phys. Lett. B 348, 29 (1995).
- [28] T. Nakamura et. al., Phys. Rev. Lett. 96, 252502 (2006).
- [29] E. Garrido, D.V. Fedorov, A.S. Jensen, Nucl. Phys. A 708, 277 (2002).
- [30] G.R. Caughlan and W.A. Fowler, At. Data Nucl. Data Tables 40, 283 (1988).
- [31] V.D. Efros, H. Oberhummer, A. Puskhin, I.J. Thompson Eur. Phys. J. A 1, 447 (1998).